

# Present and future prolonged drought impacts on a large temperate embayment: Port Phillip Bay, Australia

Randall S. Lee · Kerry P. Black · Cyprien Bosserel ·  
Dougal Greer

Received: 31 January 2011 / Accepted: 12 March 2012 / Published online: 26 April 2012  
© Springer-Verlag 2012

**Abstract** Observations of a large temperate embayment in Victoria, Australia, reveal a sustained climatic shift that occurred in response to a prolonged drought in the region during 1997–2009. Historically, the bay is fresher than the ocean with fresh outflow to the sea. However, the drought has caused substantially elevated salinity and temperatures above adjacent oceanic waters. The bay's capacity to dilute and flush waste discharges to the ocean was also changed. Observed conditions have been numerically modelled with hydrodynamic and coupled lagrangian particle dispersion models to test differences in dispersion and exchange during historically fresher conditions and hypersaline bay scenarios. Further scenarios were tested for projected climate conditions which were similar to the recent drought responses in the bay. The models identified the effects on the circulation

of the climatic shift including regions of increased vulnerability to extreme salinity in the bay, with some existing discharges concentrating in these regions of heightened vulnerability. Absolute salinity in the bay could reach critical levels of over  $38 \text{ g kg}^{-1}$ , in places, which may compromise bay ecology.

**Keywords** Hypersaline · Embayment · Catchment discharge · Climate change · Drought

## 1 Introduction

Typically, a sea that is mostly enclosed and has limited exchange with adjacent oceans, due to an entrance sill, is defined as Mediterranean (Tomczak and Godfrey 1994). Here, the water circulation is dominated by salinity and temperature differences rather than winds. These seas typically fall into two categories. Those that act as concentration basins where evaporation dominates and the fresher ocean enters the bay in the surface layer, and those that act as dilution basins where significant catchment inflows drive a surface layer outflow to the ocean. Concentration basins are typically noted in the tropics and sub-tropics where evaporative fluxes perennially or seasonally override precipitation. Known examples of these include Laguna Madre in the Gulf of Mexico (Tunnell and Judd 2002), San Diego Bay (Largier et al. 1996), the Guadiana estuary in Portugal–Spain (Domingues et al. 2011), Lagoa de Araruama in Brazil (Souza et al. 2003) and Shark Bay in Australia (Nahas et al. 2005).

Port Phillip Bay in Southern Victoria, Australia (Fig. 1), provides an interesting case for a temperate marine system sensitive to climatic variations. Although the bay is large in area ( $2,000 \text{ km}^2$ ), its hydrodynamics are constrained by a

---

Responsible Editor: Chari Pattiaratchi

---

This article is part of the Topical Collection on *Physics of Estuaries and Coastal Seas 2010*

---

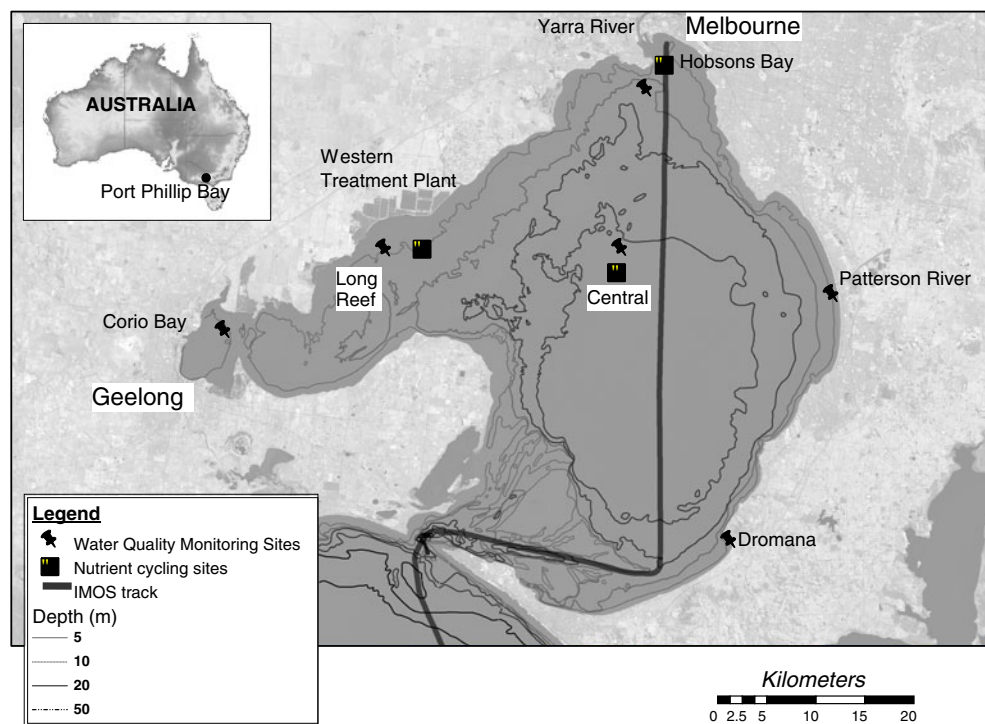
R. S. Lee (✉)  
Environment Protection Authority,  
Melbourne, Victoria, Australia  
e-mail: randall.lee@epa.vic.gov.au

K. P. Black  
University of Melbourne,  
Melbourne, Victoria, Australia  
e-mail: kerrypeterblack@yahoo.com

C. Bosserel  
University of Western Australia,  
Perth, Australia  
e-mail: bosserel@sese.uwa.edu.au

D. Greer  
ASR Pty Ltd,  
Raglan, New Zealand  
e-mail: D.greer@asrltd.co.nz

**Fig. 1** Locality map of Port Phillip Bay, Australia, showing bathymetry, sampling sites, key catchment inflows and survey tracks used in this paper



relatively small entrance and extensive neighbouring flood-tidal sand banks (Black et al. 1993). The combination of these entrance features reduces tidal volumes by more than 90 % and induces long residence times within the bay of up to 2 years. The density structure of this large bay is not so much dominated by the flushing through the entrance. These entrance features act as a sill, which result in a critical balance between surrounding catchment inflows and within-bay evaporative fluxes, and thus can be defined as a system with Mediterranean characteristics. Hearn et al. (1996) indicate that for the temperate marine conditions in Tomales Bay, the observed seasonal dominance of catchment inflow and evaporation resulted in a seasonally inverse estuary during summer. During such periods, the bay flushing times increased, a feature observed for many Mediterranean estuaries (Aubrey and Friedrichs 1996).

For Port Phillip Bay, the Yarra River and the Western Treatment Plant provide the majority of freshwater inflow that typically overrides the evaporative capacity of the bay and maintains fresher-than-ocean conditions (hyposaline). With catchment loading primarily at the northern end of the bay, the salinity gradient typically becomes more salty towards the southern open entrance as anticipated.

However, Port Phillip Bay monitoring since 1947 indicates that during strong and prolonged (decadal) periods of drought, the bay salinities can substantially exceed ocean values, thereby reversing the normal density gradients and creating hypersaline conditions in the bay and its western arm (Brown and Davies 1991). As such, this climatically

prolonged behaviour differs from the seasonally hypersaline systems that are more typically reported for Mediterranean estuaries (Aubrey and Friedrichs 1996).

The Port Phillip Bay and surrounding region experience a temperate oceanic climate, dominated by cool wet winters and warm dry summers. The annual rainfall and mean maximum temperature data from Melbourne (Figs. 2 and 3), located in the north of Port Phillip Bay, show the region experiences cyclic 10- to 20-year inter-annual variability. The rainfall data indicate the period 1997–2009 is the most prolonged drought condition for the region since records began in 1856. Temperature records appear inversely related to the rainfall oscillations, although with the recovery in 2010 of rainfall, temperature still retains a significant positive departure from the 30-year median. Decreases in rainfall have been observed during the traditionally wetter winter–spring period, whereas the summer rainfalls have marginally increased.

Unbroken salinity records dating back to 1985 (Fig. 4) indicate an unprecedented hypersaline condition in Port Phillip Bay associated with the 1997–2009 drought that was triggered by the strong 1997/1998 El Niño. Persistently higher rainfall experienced in 2010 eventually returned the bay to a hyposaline condition in late November 2010 (Fig. 5). This unprecedented drought period thus provides an interesting parallel to projected climate change conditions for the region, which is the key focus of this paper. During this period, average rainfall reduced by ~20 % for the region, causing extreme reductions in water supply which motivated water restrictions and the construction of

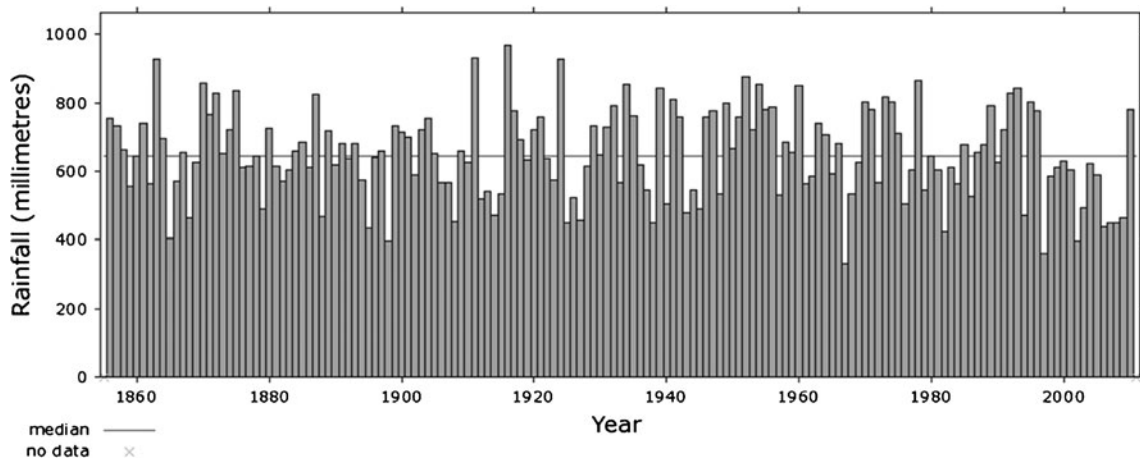


**Fig. 2** Long-term annual rainfall for Melbourne located at the northern end of Port Phillip Bay (source: station code: 86071, Australian Bureau of Meteorology)

a desalination plant to ensure ongoing domestic supply. Reductions of ~25 % in rainfall for the region by 2070 have been projected as a consequence of climate change (Whetton and Power 2007). Climate change forecasts suggest that droughts around Port Phillip Bay may become more extreme and prolonged (Whetton and Power 2007). This indicates that the hypersaline condition currently experienced in Port Phillip Bay would be expected to become well established and further enhanced. At the same time, drought conditions are exacerbated by freshwater recycling for farming that further reduces freshwater inputs to the bay. Thus, the experience in Port Phillip Bay could be considered an indicator of the likely impacts from climate change on similar large temperate estuaries globally. The impact of this significant climatic event in Australia has recently been documented for Hervey Bay in southern Queensland (Gräwe et al. 2010).

After a transition from hyposaline to hypersaline, the mixing dynamics of Port Phillip Bay are expected to be substantially changed. Coastal discharges could become more constrained to the coast within the bay. In turn, so would the bay temperatures, chemical content, evaporative fluxes, in/outflows, etc. Such climatic changes could impact on drifting fish larvae, water quality and bay ecology (Roessig et al. 2004; Boyer et al. 2009). This paper considers the hydrodynamic changes in the context of modern day dynamics and under climate change scenarios.

The goal is to determine if the circulation and flushing times will be substantially changed. If so, a key question is whether Port Phillip Bay has self-righting hydrodynamic mechanisms that might help to overcome the burden on the ecology of rising salinity. Alternatively, in the event of prolonged drought, will salinity rise to potentially dangerous thresholds that may permanently damage this highly

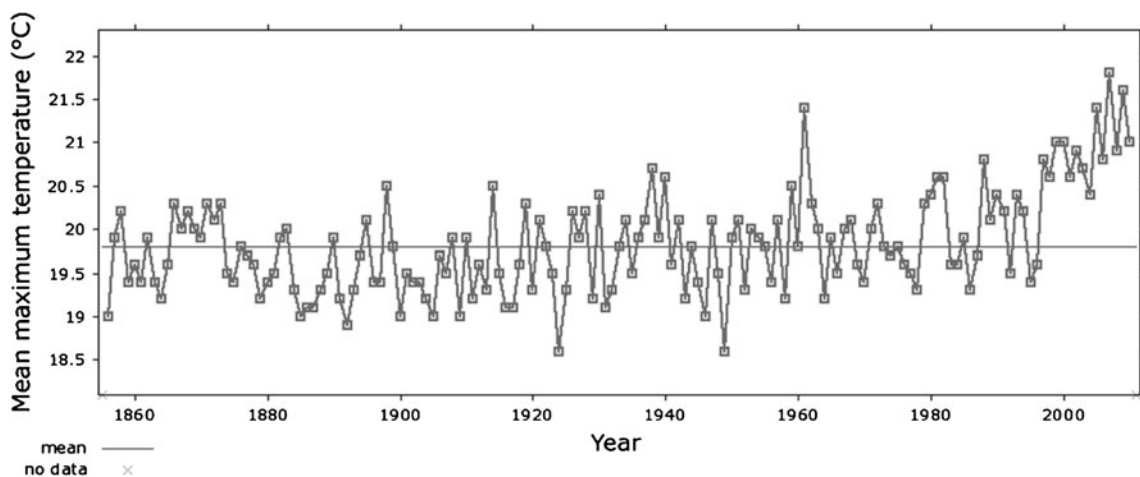
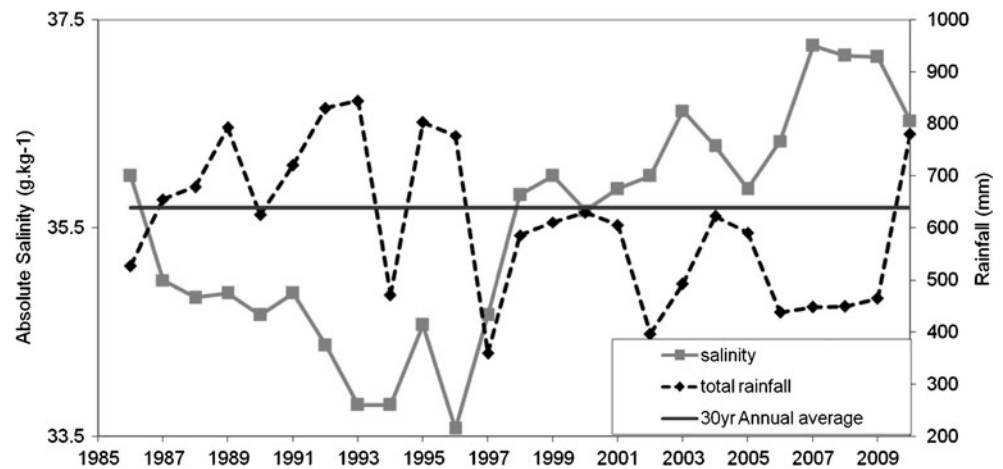


**Fig. 3** Long-term annual mean maximum temperature for Melbourne located at the northern end of Port Phillip Bay (source: station code 86071, Australian Bureau of Meteorology)

**Fig. 4** Long-term annually averaged salinity (absolute salinity) for the Central Bay site, annual rainfall for Melbourne and the 30-year (1961–1990) annual average rainfall for Melbourne. Note that salinities of  $35.6 \text{ g kg}^{-1}$  are typical of adjacent oceanic waters in Bass Strait



important water body and fishery resource? The analysis of bay-wide and ship-borne measurements (salinity/temperature) in the bay is combined with baroclinic numerical modelling to consider these questions.

## 2 Methods

With a focus on salinity in this paper, the authors have chosen to utilize the recent change to the definition of salinity according to the International Thermodynamic Equation of Seawater or TEOS-2010 (IOC et al. 2010), adopting either absolute salinity,  $S_A$  (in grams per kilogram), or practical salinity,  $S_p$ . Where salinity has been quantified through the model, the value has been calculated as absolute salinity and units provided in grams per kilogram. Where historic salinity information has been collected by instruments, the values have been provided as practical salinity using the unitless, practical salinity scale (PSS-78). According to Pawlowicz (2010), a simple comparison can be adopted for waters in the “neptunian” range ( $2 < S_p < 42$ ;  $-2 \text{ }^\circ\text{C} < T < 35 \text{ }^\circ\text{C}$ ) where

$$S_A \text{ (in grams per kilogram)} = \left( S_p \times \frac{35.16504}{35} \right) + \delta S_A, \quad (1)$$

and the correction factor,  $\delta S_A = 0$ , for coastal waters. With this assumption, numerically, the differences are essentially 0.47 %, which for the purposes of this paper (that are dealing with large salinity differences) are negligible.

Long-term measurements of salinity (along with a suite of other water quality parameters) have been made on a monthly basis at six sites around Port Phillip Bay since 1985 (EPA Victoria and Melbourne Water 2002). Figure 4 shows annual bay salinity averages (calculated as  $S_A$ ) for the period 1985–2010, during which conditions shifted (post 1997) to hypersaline, associated with a long-term drought.

Three dedicated moorings at Long Reef, Central Bay and Hobsons Bay have been operational since 2002 in Port Phillip Bay and provide hourly measurements of salinity,

temperature, chlorophyll-a fluorescence and dissolved oxygen from near-surface (3 m) and near-bottom (+3 m) sensors (Longmore and Nicholson 2010). These records are utilized for assessing decadal changes and for calibration of the stratified hydrodynamic model.

Continuous underway sampling systems have been deployed on dedicated survey vessels to map water quality (salinity, temperature, chlorophyll-a fluorescence, turbidity and nutrients) during 1992–1994 (Harris et al. 1996) and 2007–2010 (Ellis et al. 2011; Pelican Expeditions 2010). Designed around the Seabird SBE45 thermosalinograph, these sampling systems have mapped representative snapshots of the bay for the wetter conditions of 1994 and drought extremes in 2007 as observed in the long-term records (Fig. 4). These records are used to initiate model hot starts for the two observed conditions.

Autonomous sampling systems were developed by EPA Victoria during the initial 2007 survey work and then installed on the trans-Tasman ferry, the “Spirit of Tasmania I”. This ferry traverses from north to south across the bay and across Bass Strait to Tasmania each day (see ship track in Fig. 1). Since 2008, routinely mapped water quality observations of salinity (along with temperature, chlorophyll-a fluorescence and turbidity) have been available (Fig. 5). These ship-borne measurements are provided by EPA Victoria to the national Integrated Marine Observing System (IMOS 2009) for broader data distribution. The bay-wide transect is the first long-term dataset of these water quality parameters, which resolves the detailed spatial and temporal dynamics of the bay.

The receiving bay model employed for this study is Model 3DD (Black et al. 1991), a 3-dimensional salinity and temperature-stratified hydrodynamic model that incorporates an array of wind stations, sea level gauges, sea surface temperature, barometric pressure, humidity, solar radiation and cloud cover data as boundary conditions to drive the hydrodynamic environment. This model has been

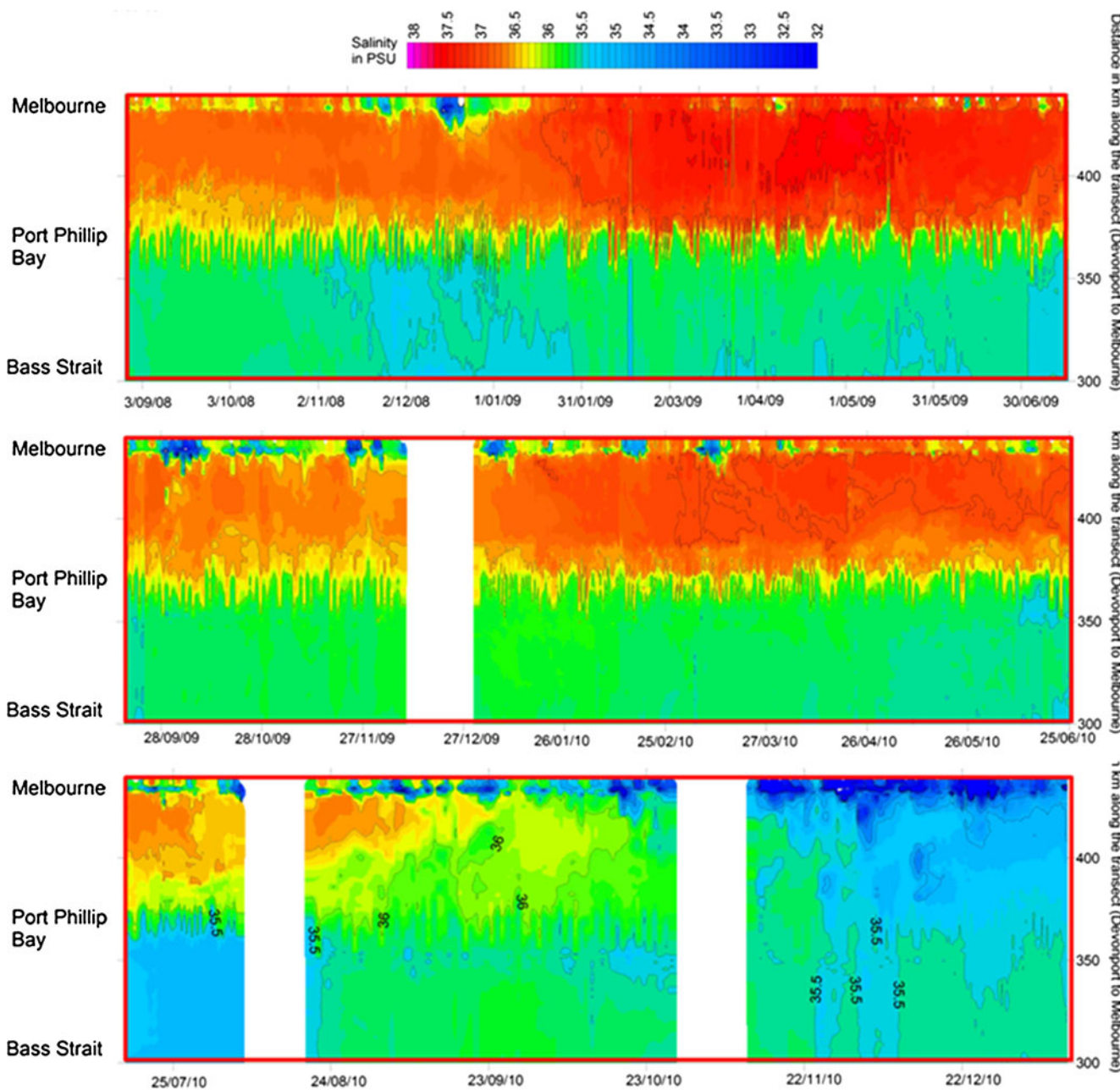


Fig. 5 2008–2010 practical salinity on the north–south passenger ferry transect through the bay (track shown in Fig. 1) (source: IMOS 2009)

regularly applied to Port Phillip Bay since 1985 (Black et al. 1993) and has been substantially calibrated in the bay and for many estuaries worldwide (Black and Gay 1987; Middleton and Black 1994; Black et al. 2005). For this study, the model was configured to run on an 800-m horizontal grid with eight layers through the water column.

The catchment inputs to the model are simulated using the “PortsE2” catchment model (Argent et al. 2007). A total of 26 unique point sources (flows and salinities from rivers and drains) are input to the 3DD model as a daily time series. Other factors including total suspended solids, total nitrogen, total phosphorous, pathogens, toxicants and litter

were incorporated into various application simulations but are not all discussed here. Numerical simulations were undertaken for the years 2004–2005 as part of a broader regional study assessing the impact of catchment inflows to local marine systems (EPA Victoria and Melbourne Water 2009).

A lagrangian particle dispersal model POL3DD (Black and Parry 1999) is used in conjunction with hydrodynamic output to assess dispersion of catchment loads and ocean exchange of larval particles (Bathgate 2010). This model seeds the domain with particles which are tracked as they move with the currents coming from the coupled

hydrodynamic model. The particle scheme uses a random walk diffusion with an eddy diffusivity of  $0.1 \text{ m}^2 \text{ s}^{-1}$ . This value is in accordance with previous detailed studies in the bay (Black and Parry 1999). Mixing is simulated by the random movements of the particles, while diffusion and mixing are also intrinsic to the prediction of the currents coming from the hydrodynamic model, and adopted in POL3DD. The time step is limited by a Courant number, whereby the time step is limited such that a particle cannot travel more than half a cell width in a single step. The model adopts a second-order particle advection scheme to allow for curvature in the flow patterns (Black and Gay 1988). The model allows particles to exhibit various “behaviours” which are commonly adopted when simulating ecological systems or fish larvae (Jenkins et al. 1999). In this paper, the simulated particles move in three dimensions and simulate fallout of suspended loads from catchment inflows and buoyant larval behaviour. The catchment inflows are provided as daily loads from the PortsE2 model output. The location of the larval releases, their relative numbers released and timing of release relate to observations of gastropod larval abundance and behaviour at marine park reef sites by Bathgate (2010).

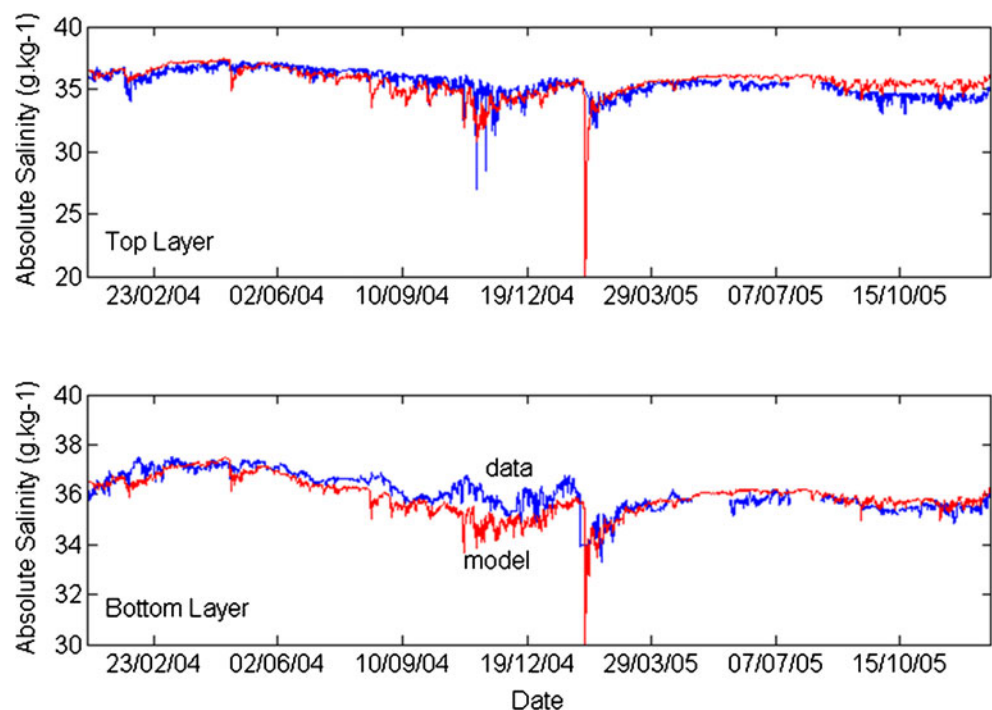
Climate change model scenarios used 2030 projections for rainfall and evaporation in the Melbourne region from the CSIRO Mk3 A1F1 medium sensitivity scenario (Whetton and Power 2007). To provide

comparative results, the 2004/2005 model rainfall and evaporation inputs were modified accordingly, but all other factors remained the same. To simulate observed (and expected future) bay hypersalinity, the receiving bay model was extended to incorporate standard evaporative flux equations based on the relative vapour pressures between the air and the sea. Evaporation is enhanced during strong winds or periods of large vapour pressure gradients.

For the modelling of water temperature due to ocean atmosphere and solar radiation exchanges, the Model 3DD adopts the full temperature flux equations augmented by a unique “nudging scheme” which uses observed satellite sea surface temperatures to “nudge” the model every 3–5 days.

A comparison of the model salinity with in situ data collected at the mooring sites is undertaken to assess the skill of the model to simulate the effectiveness of the evaporation scheme employed. There are some differences to consider in that the mooring samples hourly at specific depths (3 and 1 m off bottom), ranging vertically by  $\sim \pm 1 \text{ m}$  (given typical tide and wind wave conditions) and horizontally  $\pm 2 \text{ m}$  (given the length of the mooring line and expected current velocities). The selected model cell represents an  $800 \times 800\text{-m}$  area for a “surface” and “bottom” layer of 0–2 and 10–15 m, respectively. The resultant model predictions for salinity over a 2-year period of simulation show general agreement with the mooring data (Fig. 6), capturing seasonal cycles and most of the weather-band events.

**Fig. 6** 2004–05 absolute salinity (in grams per kilogram) comparisons of moored observations (top, –3 m, and 1 m off bottom layers) and model results at the Hobsons Bay site (11 m), within Port Phillip Bay. Note that gaps in observed data are due to mooring downtime. The mean (and variances) of observed top and bottom absolute salinity is  $35.64 (0.95)$  and  $36.30 (0.48)$   $\text{g kg}^{-1}$ , respectively



There are some periods where differences occur, notably a broad discrepancy in November 2004 and a sharp spike in February 2005. When comparing the top and bottom layers for the November 2004 period, there is an observed freshening in the surface layer that is not apparent in the bottom layer. The model appears to have overmixed the lower salinity into the bottom layer at this time, possibly due to the relative coarseness of the vertical layering in the model. The spike in February 2005 relates to a 1 in 20-year flood event delivered to the bay as an instantaneous daily load from the catchment by the PortsE2 catchment model. As such, it overestimates the initial volume delivered through the model's input boundary condition resulting in a low salinity spike ( $S_A$ ,  $\sim 20 \text{ g kg}^{-1}$ ) in the surface model layer. On subsequent days after the initial flood

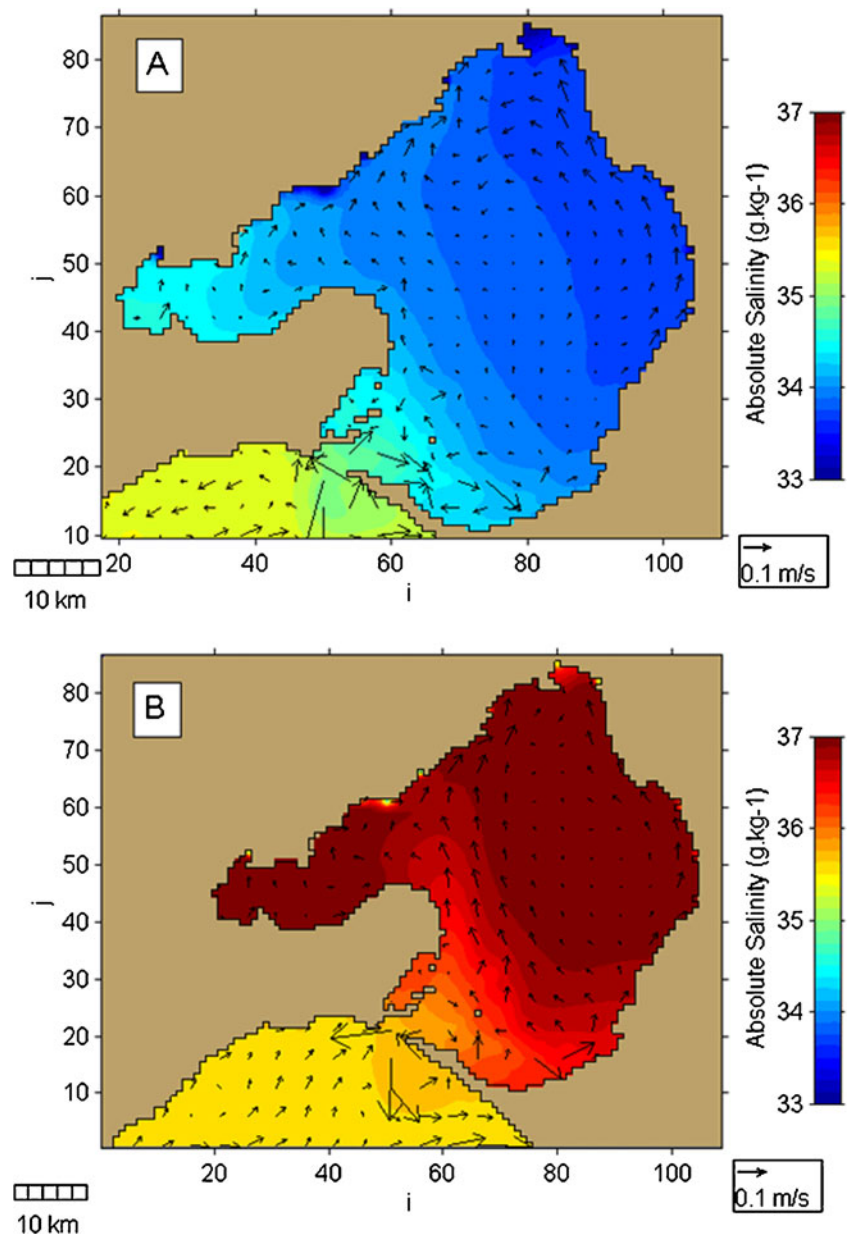
spike, the modelled bay salinity has adjusted back to match observations for the remainder of the flood recovery. As the near-surface mooring sensor is located at 3 m depth, it is likely that the salinity was less than the surface layer.

### 3 Results

#### 3.1 Measurements

Surveys undertaken during 1992–1994 (Harris et al. 1996) depicted wetter conditions with average salinities (as “ $S_A$ ” interpreted in the model) across the bay being  $\sim 2 \text{ g kg}^{-1}$  less than the adjacent oceanic water of Bass Strait (Fig. 7a). The

**Fig. 7** Port Phillip Bay salinity observations interpreted for the model along with modelled residual circulation in the surface layer associated with **a** fresh conditions during the 1992–1996 study (Harris et al. 1996) and **b** hypersaline conditions during 3–12 January 2007



hypersaline condition for Port Phillip Bay was surveyed in 2007 (Fig. 7b) where bay salinities (as “ $S_A$ ” interpreted in the model) were consistently  $1 \text{ g kg}^{-1}$  higher and up to  $2.5 \text{ g kg}^{-1}$  greater in the shallow western arm.

The subsequent ship-borne measurements (Fig. 5) reveal a consistent hypersaline condition through all seasons since the beginning of surveys in September 2008. Small pockets of lower salinity water at the start (north) of the ship track near the entrance to a large river (Yarra River) are absorbed into the overall hypersaline bay within about 5 km of the river entrance. Bay-wide salinities rose steadily from 2008 into 2009 until the highest salinities ( $S_P$  average,  $37.2 \text{ g kg}^{-1}$ ) occurred in early May 2009 at the end of a very dry summer. After above-average rainfall throughout 2010, the bay finally returned to a hyposaline state by late November 2010, coinciding with a proliferation of plankton activity responding to the enhanced nutrient inflows.

### 3.2 1994 and 2007 modelling

The observed salinity conditions from 1994 (hyposaline) and 2007 (hypersaline) surveys were assimilated into the model as hot start conditions, and then the model simulated 100 tidal cycles. In both cases, the same 2004–2005 time series boundary conditions (wind, inflows, etc.) were adopted; only the initial condition was changed. Comparisons reveal the impact of salinity on circulation associated with these two conditions. After removing initial model spin-up effects, the residual circulation in the surface layer of the model (defined as the vector average of currents in each cell over the full simulation) indicates significant changes in circulation associated with the altered salinity regime of the bay (Fig. 7).

Residual flows for the surface layer show much stronger currents heading north along the western side of the Central Bay in the hypersaline case. Net flows for the hypersaline case are stronger to the NE in the northern bay where bay salinities are highest. The salinities are essentially opposite in the two cases. In 1994, the northeast segment of the inner bay is the freshest, while this region has switched to become the most saline in 2007. In both cases, the western zone where the Corio Bay sampling site is located is more saline than the Central Bay. The western zone (known as the Geelong Arm) is a semi-enclosed embayment with correspondingly reduced flushing, and so evaporation leads to higher salinities than in open bay waters. With minimal freshwater inputs from streams, the western end of the Geelong Arm at Corio Bay is therefore highly sensitive to climate changes and droughts. To demonstrate this, time series model results are shown in Fig. 8 from a model cold start, where initial conditions are a uniform salinity,  $S_A =$

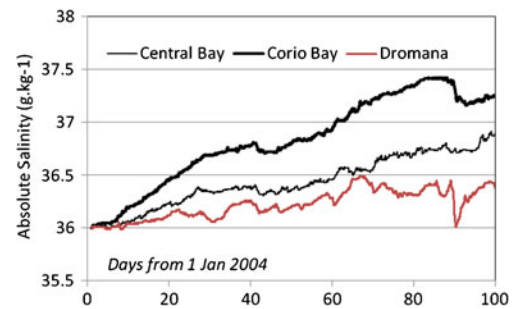


**Fig. 8** Modelled surface layer (0–2 m) absolute salinity shown as a time series extracted at locations corresponding to three observational sites in Port Phillip Bay

$36 \text{ g kg}^{-1}$ . The time series simulation of salinity from three water quality sites at Central Bay, Corio Bay and Dromana (near the bay entrance) indicates the relative response of the sites over time to their local influences of evaporation, catchment inflow and ocean exchange. The simulation is run during a period of summer heating (100 days from 1 January 2004) and shows the marked increase in salinity at Corio Bay relative to the other sites.

Focusing on the NW region of the bay where a major sewage treatment plant discharges to the bay (the Western Treatment Plant), this essentially freshwater discharge appears to be constrained by the stronger salinity gradients set up by the hypersaline bay (Fig. 9). This reduced dispersal is likely to cause increased concentration of the pollutants associated with the waste stream in the vicinity of the discharge.

In addition to the within-bay effects of hypersalinity, altered ocean exchange processes were investigated using the particle-tracking model. Representative particle releases simulating larval material from three Marine Park locations at the entrance to Port Phillip Bay were tracked (Fig. 10). Larval releases were timed for high tides during their spawning period Nov–Dec (Bathgate 2010). The hypersaline case indicates increased ranging of drift particles ( $\sim \pm 3 \text{ km}$ ) both inside and outside the bay, indicating an enhanced oceanic exchange.

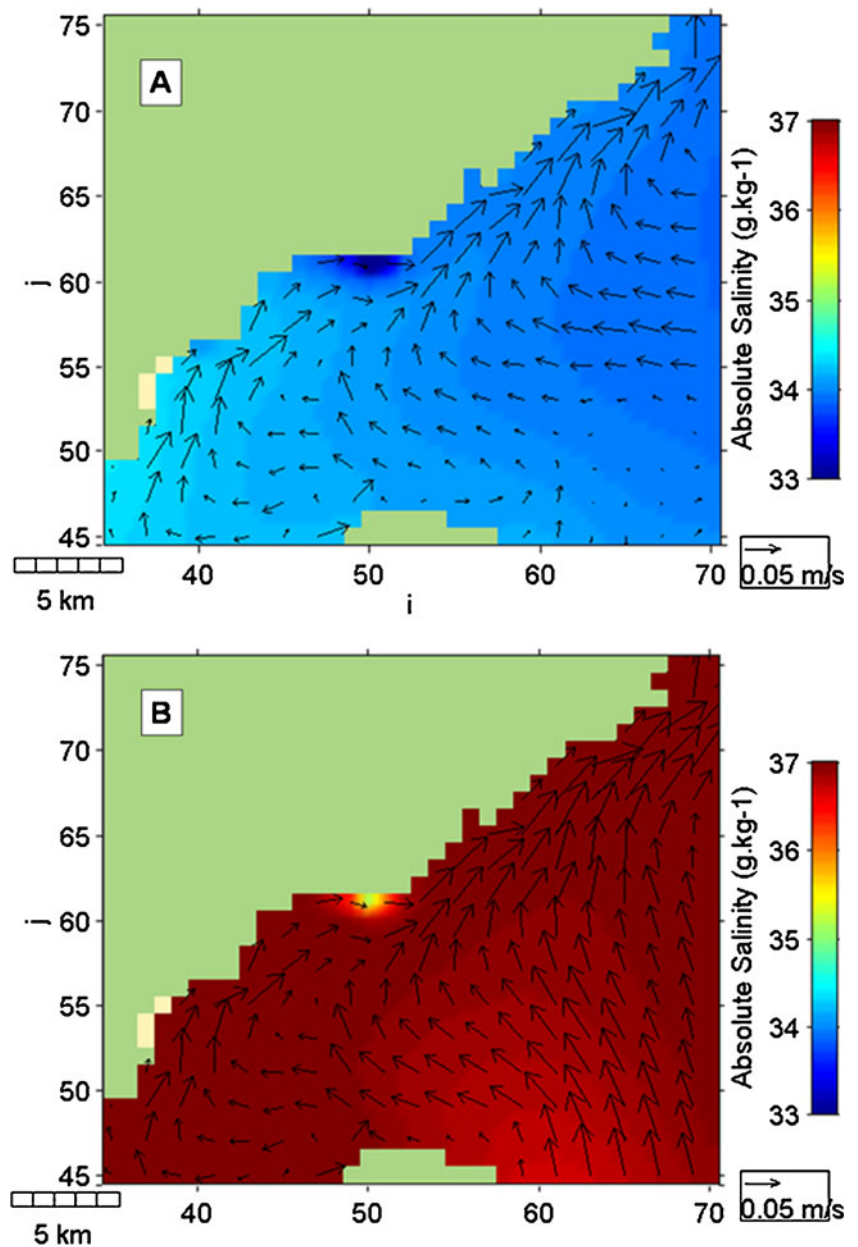
The net differences in salinity and sea level are shown in Fig. 11, where respective surface and bottom layer circulation anomalies are shown as vectors. The positive  $2\text{--}3 \text{ g kg}^{-1}$  absolute salinity anomaly in the bay is associated with a slight but noticeable negative sea level anomaly. The surface northward inflow anomaly is countered by bottom-layer southward outflows.

### 3.3 2004 and 2030 modelling projections

Bay model simulations compare a hypersaline condition, with additional 2030 climate change projections for



**Fig. 9** Averaged salinity and residual velocity in the surface layer of the model near a major sewage plant discharge (WTP) shown for **a** the 1994 hyposaline and **b** 2007 hypersaline bay condition

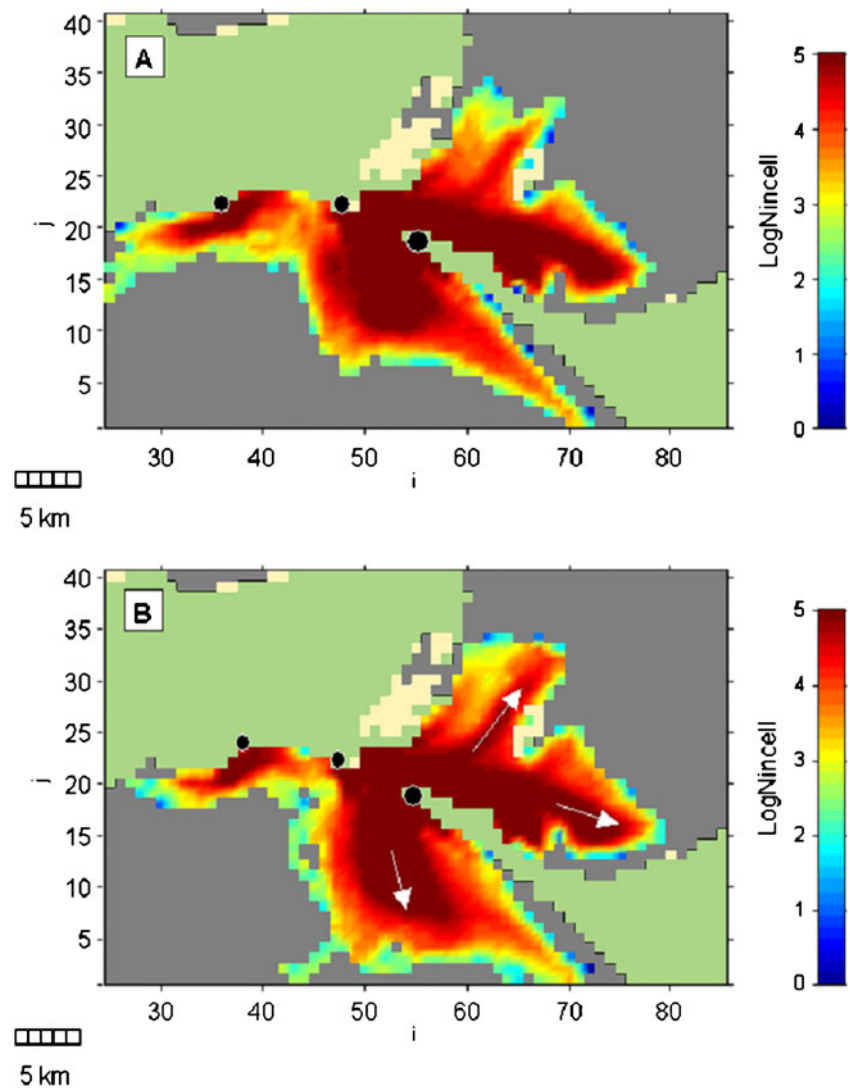


evaporation (+4.7 %) and rainfall (−2.7 %) (Whetton and Power 2007), with hyposaline conditions run with the 2004 time series. In this simulation, river flows were reduced by 2.7 % with the rainfall. Furthermore, particle dispersal simulations were undertaken to model passive transport of material from the river and are used to assess the dispersion of load coming from the major river catchment (Yarra River) in the north. As catchment loads are represented as proportional to flow in the PortsE2 catchment model, the 2030 scenario loads to the bay were reduced. Figure 12 indicates significant reductions in catchment load and reduced dispersion of the catchment outflow for the 2030 projection. A north-east contraction of the fallout footprint from the Yarra

discharge is the result of the enhanced northward flows observed in the model surface layer in the hyposaline condition combined with the reduced flow (~10 %) from the rivers. This is highlighted by the residual salinity and circulation differences (Fig. 13). It is likely that this net northward inflow is associated with the increased evaporation and reduced catchment inflow. While an exchange of bay volumes can be either induced by tides or evaporation, the flushing of buoyant particles from the bay requires oceanic exchange.

The particle-tracking model Pol3DD was used to assess flushing for these two climatic conditions. In all cases, the entire bay was filled with particles and allowed to drift throughout the simulation. As particles

**Fig. 10** Using field gastropod release numbers (Bathgate 2010), lagrangian particle dispersion models were run for ~2 months with larval releases on every high tide at three locations near the entrance to Port Phillip Bay (shown by *black dots*). The integrated number of particles ( $\log_{10}$ ) that have been counted per cell for the 2 months are shown for **a** hyposaline and **b** hypersaline cases. Land is shown as *green*, intertidal areas as *beige* and water (with no particle visits) as *grey*

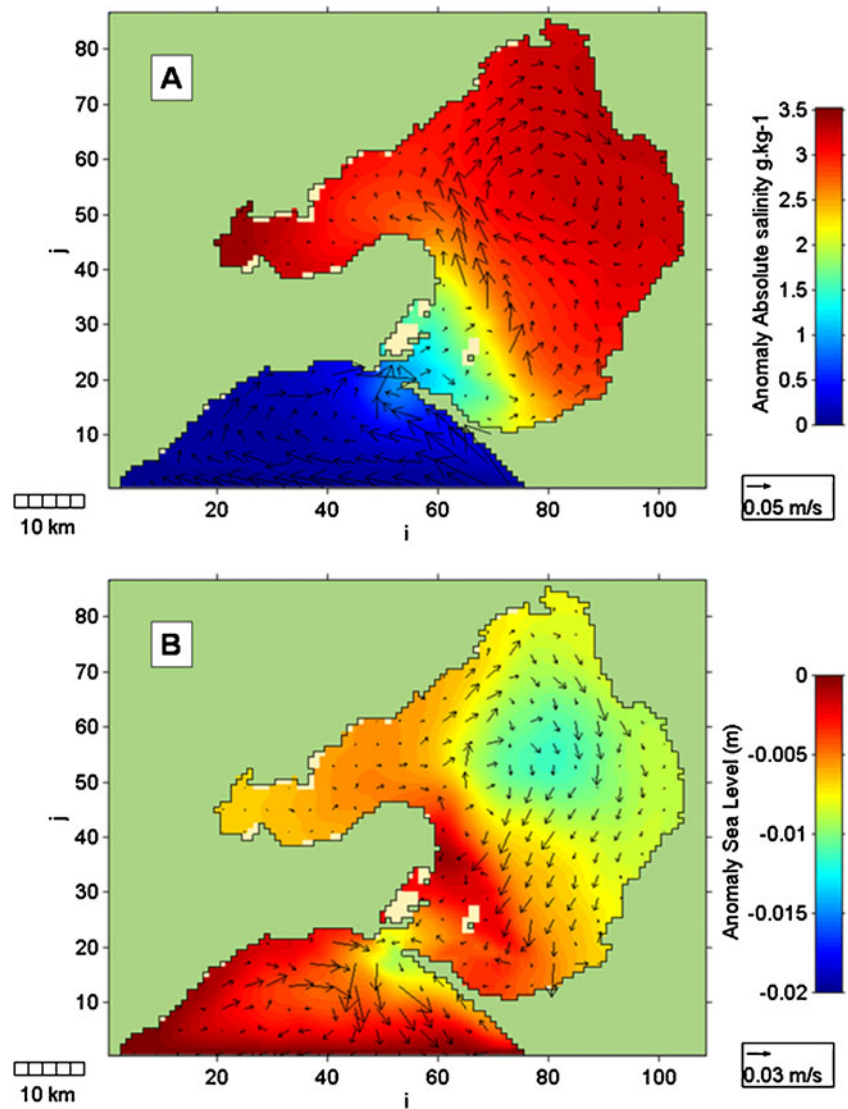


exit the bay, they are counted and removed from the simulation. For example, Fig. 14 shows a box where particles are counted and removed from the Port Phillip Bay simulations. Also, at every time step, the total number of particles remaining in the model grid is calculated. This enables a time history analysis of particle flushing. By fitting the flushing rates over the time history to exponential decay curves, the range of T90 times (time for 90 % of particles to be flushed) is approximated in Fig. 15. This rate varies as a function of both seasonal wind conditions and freshwater load variations. The results indicate that the bay flushes faster (T90 is less) for the 2030 hypersaline conditions. The values centre on 603 days (1.65 years) which is compatible with previous estimates of bay flushing times (Harris et al. 1996). Notably, by removing particles at the entrance, no particles can re-enter the bay which means that predicted flushing rates are possibly faster in the model than in reality.

#### 4 Discussion

Modelling and observations show that the salinity of Port Phillip Bay is very sensitive to the balance between rainfall and evaporation. With the onset of drought, the bay was shown to transition between hypersaline and hyposaline with some very substantial changes of mean absolute salinity with up to  $4\text{-g kg}^{-1}$  variation over the last two decades (Fig. 4). The model has shown this occurs because of the very long residence times of bay waters (T90 values of nearly 2 years) and because rainfall and evaporation are approximately equal during mean conditions. Thus, Port Phillip Bay is likely to be impacted under a changed climate which is predicted to exhibit a substantially greater likelihood and duration of droughts punctuated with (an increase in) intense summer storms such as the one experienced in early February 2005. Climate projections for other large temperate embayments such as Chesapeake Bay

**Fig. 11** Mean difference plots of **a** surface salinity and currents, and **b** sea level and bottom layer currents for the hypersaline minus the hyposaline cases. The anomalies show increased inflow at the surface and outflow at the seabed during hypersaline conditions



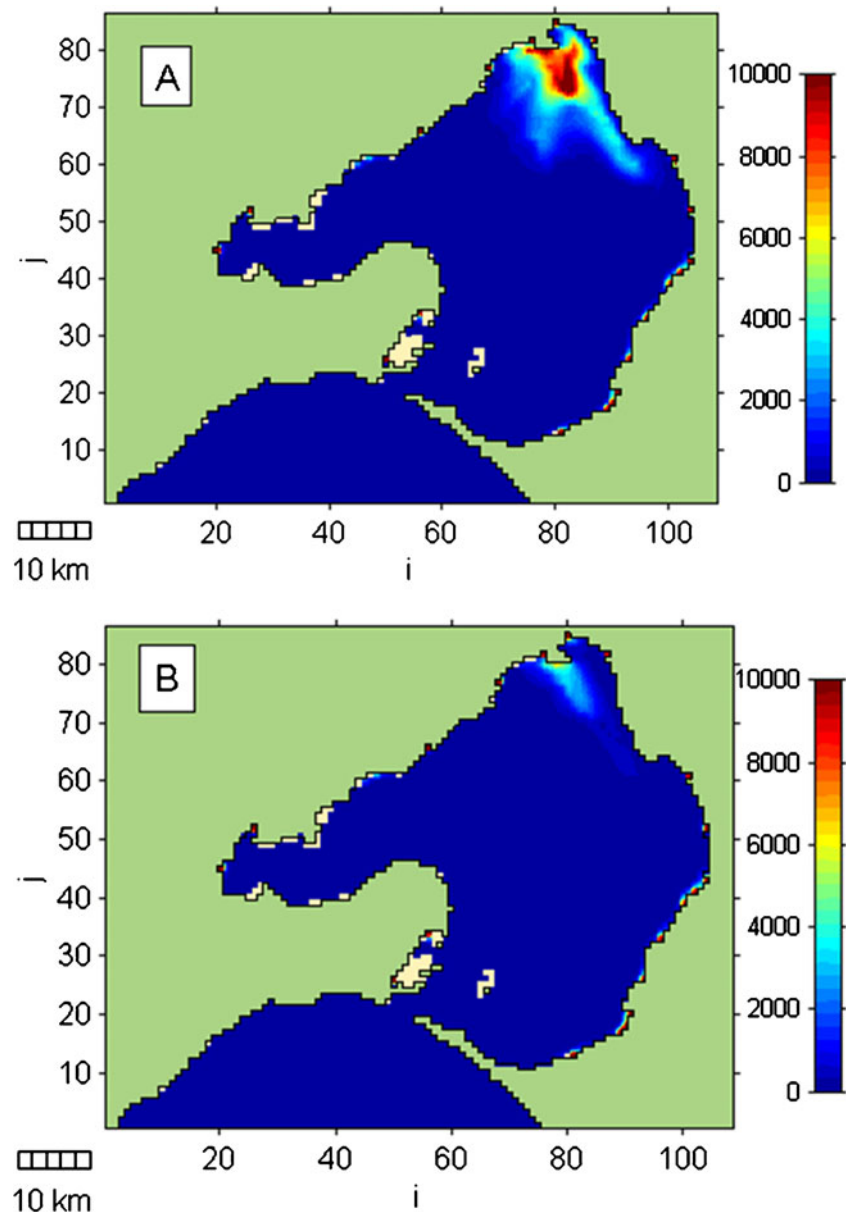
(Najjar et al. 2010) suggest with significant variations in catchment inflow (due to increases in extreme events) will enhance salinity variability that will stress stocks of seagrass and favour uptake in the water column by plankton.

Climate change scenarios for 2030 indicated that enhancements in salinity were associated with the decreases in rainfall and enhanced evaporation, but other factors will also play a role. For example, the discharge of concentrated re-use waste in a future climate-modified system is likely to further compound the risk of pollutant accumulation and impact in the vicinity of the discharge. Altered bay circulation has implications for dispersal of terrestrial nutrients to existing fish nurseries and the exchange of biota with the adjacent ocean, potentially reducing connectivity of this system. The study suggests coupled modelling of catchment

discharges, and a dynamic receiving marine environment provides insight into the management of sustainable limits for a climate-modified system. It also helps identify localized impacts that may require additional focus for management.

For Port Phillip Bay, the highest salinity occurs at Corio Bay in the western end of the Geelong Arm, as noted by both model projections and observed drought conditions. In places, absolute salinities could exceed 38 g kg<sup>-1</sup>, which may be critically high for some species and larvae (Fielder et al. 2005; Booth et al. 2009; Last et al. 2010). A more extreme example of hypersaline impacts on a large embayment scale has been observed in Florida Bay which is of similar size (2,200 km<sup>2</sup>) to Port Phillip Bay, but shallower and influenced by a tropical climate. Here, absolute salinities can reach up to 41 g kg<sup>-1</sup> at the end of a

**Fig. 12** Settled particles associated with **a** hyposaline bay and existing catchment flow (2004) and **b** 2030 projected hypersaline bay with future catchment flows



drought period (Kelble et al. 2007) and have coincided with seagrass die-off and an increase in algal blooms (Boyer et al. 2009). Similarly, Ball et al. (2009) has observed a significant reduction in seagrass coverage in the Geelong Arm of Port Phillip Bay coinciding with the 1997–2009 drought period.

Port Phillip Bay can only overcome the predicted salinity rises due to drought through flushing exchanges of saline waters with ocean inputs. But many factors determine the residence times of a bay, including the fraction of volume dispelled through the entrance by tides each cycle, evaporation, freshwater inputs and bay mixing capacity. Moreover, the residence time of bay water may be very different to the residence time of

dissolved substances because the water can evaporate while the dissolved substances such as salt or pollutants may remain trapped. The prolonged drought response in Port Phillip Bay has been shown to cause significant changes to salinity and the associated circulation patterns. We ask if the altered dynamics and flushing rates reinforce or oppose the salinity increases to either exacerbate or diminish the predicted climate change impacts on Port Phillip Bay.

One might initially assume that greater evaporation and reduced freshwater inputs to the bay (which cause greater net inflow through the entrance) should lead to correspondingly reduced flushing of material from the bay. On the contrary, however, the modelling shows that there is greater

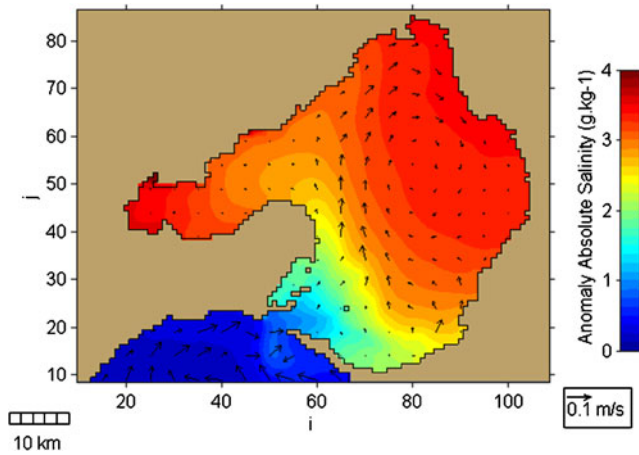


**Fig. 13** Mean surface layer salinity (absolute salinity) and circulation anomalies in Port Phillip Bay between 2004/2005 and 2030 simulations

dispersal of material at the entrance (Fig. 10) and shorter T90 values (Fig. 15) signifying faster flushing for the hypersaline case in 2030. Thus, the stratified 3D model is showing that the altered density-driven circulation patterns in 2030 are somehow overcoming the net inflow effect, even though the influence of gravitational circulation is shown to be small in Fig. 11; the T90 values are only slightly different in the two cases.

The effect of hypersalinity may be better understood using a notional two-box model analogy. The “Ocean” box is essentially constant in salinity while the “Bay” box varies

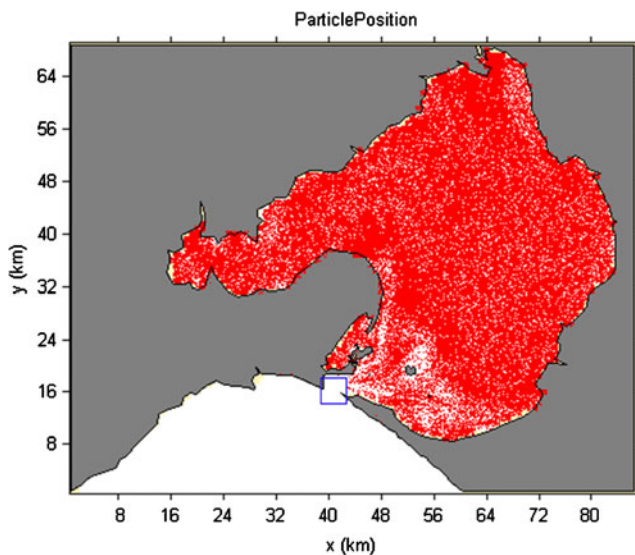
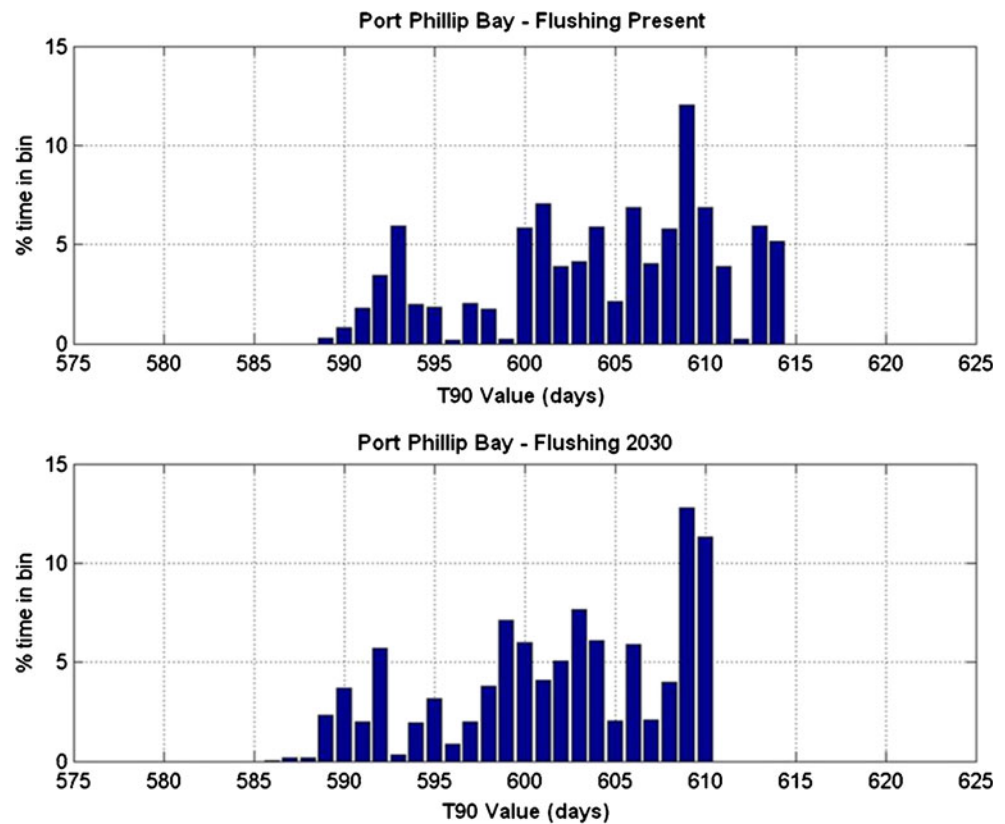


**Fig. 14** Port Phillip Bay model filled with drifting particles. At each time step, particles within the entrance box are counted and removed from the simulation (representing fresh source water), and the total number of particles in the model grid is counted

from less to more saline than the ocean, i.e., hyposaline to hypersaline. In the hypersaline case, the higher density of the bay would induce gravitational currents that should lead to enhanced outbound flows at the seabed and inbound at the sea surface. Figure 11 shows that this is indeed occurring, when the 1994 and 2007 conditions are compared. Thus, as the salinity climbs, the near-bed currents are enhanced, and the bay tends to flush more quickly at the seabed. The flushed volume is replaced by inflows at the surface which also enhances flushing. A similar mechanism, but more pronounced, is observed in the gulfs of South Australia where very saline water from the upper reaches due to evaporation is flushed from the gulfs as a density current at the seabed (de Silva Samarasinghe and Lennon 1987). Recent observations have also been made (Gräwe et al. 2010) in Hervey Bay on the east Australian coast, where adjustments in salinity (more subtle than Port Phillip Bay) occurred in response to the prolonged 1997–2009 drought. The authors found that salinity flux from the bay had increased, and the evaporation-induced residual circulation had accelerated, much as the models suggest in this study. This is contrary to seasonal variations observed by Hearn et al. (1996) in Tomales Bay, where the summer hypersalinity was found to be associated with longer flushing times. In the smaller Tomales Bay, Hearn et al. (1996) showed that rainfall was much higher in winter than summer, and flushing was correspondingly faster in winter. Hence, for larger systems such as Port Phillip Bay and Hervey Bay, prolonged evaporative dominance over catchment inflows reaches sustained hypersalinity, which (due to the larger bay size) is not achieved with more moderate seasonal forcing.

In principle, Port Phillip Bay has a self-sustaining mechanism that may prevent salinities rising endlessly in proportion to reductions in rainfall and river inputs. However, this flushing mechanism relies on rather large increases in the bay’s salinity to be effective. The current changes shown in Fig. 11 are quite small even when absolute salinity differences between the hypersaline and hyposaline conditions exceed  $\sim 3 \text{ g kg}^{-1}$ . Of course, such rises can be detrimental to marine life, and impacts might still be anticipated on zooplankton growth, dispersal of species, phytoplankton growth, nutrient inputs and productivity. Moreover, on the extensive Sands region inside the entrance, strong currents of around  $0.8\text{--}1.0 \text{ m s}^{-1}$  (Black et al. 1993) induce substantial mixing of the upper and lower layers. This breaks down the vertical stratification and greatly inhibits the outbound bottom flows in this region (Fig. 11), where the residual currents are slow compared to those in the bay. Indeed, the mechanism is inhibited during strong tidal mixing in many bays, including Shark Bay

**Fig. 15** Distribution of Port Phillip Bay T90 residence times (in days) throughout the 2004 (*top panel*) and 2030 (*bottom panel*) flushing simulations. Simulations based on the flushing of a conservative tracer from the bay



(Nahas et al. 2005; Smith and Atkinson 1983). In the context of the notional two-box model, Port Phillip Bay is complicated by a high mixing zone which slows and inhibits the simple mechanism of outbound bottom flow due to gravitational circulation in the hypersaline case.

During the opposite hyposaline conditions, the same concepts apply except that the circulation is reversed. Flows are expected to be more generally outbound at the surface and inbound at the seabed. Such circulation helps to eliminate the river water from the bay. Of course, vertical mixing due to overturning (coastal up/downwelling), turbulence and horizontal mixing can cause the gravity currents to be mostly negated, and residence times are then primarily related to the fraction of volume dispelled each tidal cycle through the entrance and the horizontal mixing dynamics over the Sands region (Black et al. 1993). In Port Phillip Bay, the model shows a strengthening of the advective circulation that rotates clockwise around the Central Bay region and helps to carry water from the upper bay to the entrance where flushing may occur (Fig. 11).

Other factors such as temperature variations will also alter the density structure. The bay experiences seasonal temperature variations of 10–20 °C which are larger than the 13–18 °C range in the adjacent ocean, so seasonality of the resultant density occurs with strongest gradients in

winter. However, the density differences due to temperature are far smaller than those associated with salinity variations. Consequently, while temperature influences bay circulation, the bay flushing is more dependent on wind, tides and salinity gradients.

This study has shown that Port Phillip Bay can be classified as vulnerable in relation to climate change, partly due to its long residence times. Substantial increases in salinity are anticipated to occur (particularly in the Geelong Arm), and these are sufficient to alter the marine ecology, either permanently or cyclically. Further studies of the relationship between salinity, primary production and larval recruitment are needed to fully understand the potential ecological impacts.

**Acknowledgments** This work was borne from an earlier project that was funded by the National Department of Environment and Heritage to develop bay and catchment models for the Port Phillip Bay and Western Port region. The authors wish to thank Shaun Harrison, Sebastien Mancini, Guillaume Martinez, Rachael Bathgate and Andy Longmore for their contributions to the background of this paper.

## References

Argent R, Pexton HM, McAlister AB (2007) The PortsE2 decision support system—an application of E2, In: Oxley L, Kulasiri D

- (eds) MODSIM07 international congress on modelling and simulation: Christchurch, New Zealand, Modelling and Simulation Society of Australia and New Zealand. pp 895–901. At: [http://www.mssanz.org.au/MODSIM07/papers/15\\_s37/ThePortsE2\\_s37\\_Argent.pdf](http://www.mssanz.org.au/MODSIM07/papers/15_s37/ThePortsE2_s37_Argent.pdf). Accessed 27 June 2011
- Aubrey DG, Friedrichs CT (eds) (1996) Buoyancy effects on coastal and estuarine dynamics. *Coast Estuar Stud*, 53, 360p AGU, Washington, D.C., doi:10.1029/CE053
- Ball D, Soto-Berelov M, Young P, Coots A (2009) Baywide Seagrass Monitoring Program—historical seagrass mapping. Fisheries Victoria Technical Report Series No. 70. At: [http://www.oem.vic.gov.au/Assets/809/1/HistoricalSeagrassMapping\\_10Dec09\\_Final.pdf](http://www.oem.vic.gov.au/Assets/809/1/HistoricalSeagrassMapping_10Dec09_Final.pdf). Accessed 27 June 2011
- Bathgate R (2010) Connectivity in marine invertebrate populations and the role of marine protected areas. PhD dissertation, University of Melbourne
- Black KP, Gay SL (1987) Eddy formation in unsteady flows. *J Geophys Res* 92(C9):9514–9522
- Black KP, Gay SL (1988) A numerical scheme for determining trajectories in particle models. In: Bradbury R (ed) *Acanthaster* and the coral reef: a theoretical perspective. Lecture notes in Biomathematics, Springer-Verlag, pp 151–156
- Black KP, Parry GD (1999) Entrainment, dispersal and settlement of scallop dredge sediment plumes: field measurements and numerical modelling. *Can J Fish Aquat Sci* 56:2271–2281
- Black KP, Moran PJ, Hammond LS (1991) Numerical models show coral reefs can be self-seeding. *Mar Ecol Prog Ser* 74:1–11
- Black KP, Hatton D, Rosenberg M (1993) Locally and externally driven dynamics of a large semi-enclosed embayment in Southern Australia. *J Coast Res* 9(2):509–538
- Black KP, Oldman J, Hume T (2005) Dynamics of a 3-dimensional, baroclinic, headland eddy. *NZ J Mar Fresh Res* 39:91–120
- Booth D, Edgar G, Figueira W, Jenkins G, Kingsford M, Lenanton R, Thresher R (2009) Temperate coastal and demersal fish and climate change. In: Poloczanska ES, Hobday AJ, Richardson AJ (eds) *A marine climate change impacts and adaptation report card for Australia 2009*. NCCARF Publication 05/09, ISBN 978-1-921609-03-9, pp 1–19
- Boyer JN, Kelble CR, Ortner PO, Rudnick DT (2009) Phytoplankton bloom status: chlorophyll a biomass as an indicator of water quality condition in the southern estuaries of Florida, USA. *Ecol Ind* 9(6):S56–S67
- Brown V, Davies R (1991) The environmental water quality of north-western Port Phillip Bay. Melbourne Water environmental Services Technical Report, 91/005
- de Silva Samarasinghe JR, Lennon GW (1987) Hypersalinity, flushing and transient salt-wedges in a tidal gulf—an inverse estuary. *Estuar Coast Shelf Sci* 24(4):483–498
- Domingues RB, Anselmo TP, Barbosa AB, Sommer U, Galvão HM (2011) Nutrient limitation of phytoplankton growth in the freshwater tidal zone of a turbid, Mediterranean estuary. *Estuar Coast Shelf Sci* 91(2):282–297
- Ellis PS, Shabani AMH, Gentle BS, McKelvie ID (2011) Field measurement of nitrate in marine and estuarine waters with a flow analysis system utilizing on-line zinc reduction. *Talanta* 84(1):98–103
- Fielder DS, Bardsley WJ, Allan GL, Pankhurst PM (2005) The effects of salinity and temperature on growth and survival of Australian snapper, *Pagrus auratus* larvae. *Aquac* 250(1–2):201–214
- Gräwe U, Wolff JO, Ribbe J (2010) Impact of climate variability on an East Australian Bay. *Estuar Coast Shelf Sci* 86:247–257
- Harris G, Bately G, Fox D, Hall D, Jernakoff P, Molloy R, Marray A, Newell B, Parslow J, Skyring G, Walker S (1996) Port Phillip Bay environmental study final report. CSIRO, Canberra
- Hearn CJ, Largier JL, Smith SV, Plant J, Rooney J (1996) Effects of changing bathymetry on summer buoyancy dynamics of a shallow Mediterranean estuary; Tomales Bay California. In: Aubrey DG and Friedrichs CT (eds) *Buoyancy effects on coastal and estuarine dynamics*. *Coast Estuar Stud* 53:243–253
- IMOS (2009) Integrated marine observing system, Ships of Opportunity Facility. At: <http://imos.org.au/soop.htm>. Accessed 27 June 2011
- IOC, SCOR, IAPSO (2010) The international thermodynamic equation of seawater—2010: calculation and use of thermodynamic properties. Intergovernmental Oceanographic Commission, Manuals and Guides No. 56, UNESCO. 196 pp
- Jenkins GP, Black KP, Keough MJ (1999) The role of passive transport and the influence of vertical migration on the pre-settlement distribution of a temperate, demersal fish: numerical model predictions compared with field sampling. *Mar Ecol Prog Ser* 184:259–271
- Kelble CR, Johns EM, Nuttle WK, Lee TN, Smith RH, Ortner PB (2007) Salinity patterns of Florida Bay. *Estuar Coast Shelf Sci* 71(1–2):318–334
- Largier JL, Hearn CJ, Chadwick DB (1996) Density structures in low flow estuaries. In: Aubrey DG and Friedrichs CT (eds) *Buoyancy effects on coastal and estuarine dynamics*. *Coast Estuar Stud* 53: pp 227–241
- Last PR, White WT, Gledhill DC, Hobday AJ, Brown R, Edgar GJ, Pecl G (2010) Long-term shifts in abundance and distribution of a temperate fish fauna: a response to climate change and fishing practices. *Glob Chang Biol*. doi:10.1111/j.1466-8238.2010.00575.x
- Longmore A, Nicholson G (2010) Baywide nutrient cycling (denitrification) monitoring program milestone report no. 11 (June–September 2010). Fisheries Victoria Technical Report Series No. 118. At: [http://www.oem.vic.gov.au/Assets/957/1/NutrientCyclingMilestoneRep11\\_22Dec10\\_Final.pdf](http://www.oem.vic.gov.au/Assets/957/1/NutrientCyclingMilestoneRep11_22Dec10_Final.pdf). Accessed 27 June 2011
- EPA Victoria and Melbourne Water (2009) Better bays and waterways: a water quality improvement plan for Port Phillip Bay and Westernport region. Report to the Australian Government. At: <http://www.epa.vic.gov.au/water/coasts/betterbays.asp>. Accessed 27 June 2011
- Middleton JF, Black KP (1994) The low frequency circulation in and around Bass Strait: a numerical study. *Cont Shelf Res* 14(13/14):1495–1521
- Nahas EL, Pattiaratchi CB, Ivey GN (2005) Process controlling the position of frontal systems in Shark Bay, Western Australia. *Estuar Coast Shelf Sci* 65:463–474
- Najjar RG, Pyke CR, Adams MB, Breitburg D, Hershner C, Kemp M, Howarth R, Mulholland MR, Paolisso M, Secor D, Sellner K, Wardrop D, Wood R (2010) Potential climate-change impacts on the Chesapeake Bay. *Estuar Coast Shelf Sci* 86(1):1–20
- Pawlowicz R (2010) What every oceanographer needs to know about TEOS-10 (The TEOS-10 Primer). At: [http://www.teos-10.org/pubs/TEOS-10\\_Primer.pdf](http://www.teos-10.org/pubs/TEOS-10_Primer.pdf). Accessed June 2011
- Pelican Expeditions (2010) Two bays <http://www.svpelican.com.au/2bays/science.html>. Accessed 31 January 2011
- Roessig JM, Woodley CM, Cech JJ, Jr JJ, Hansen LJ (2004) Effects of global climate change on marine and estuarine fishes and fisheries. *Rev Fish Biol Fish* 14:251–275
- Smith SV, Atkinson MJ (1983) Mass balance of carbon and phosphorus in Shark Bay, Western Australia. *Limnol Oceanogr* 28:625–639
- Souza MFL, Kjerfve B, Knoppers B, de Souza WFL, Damasceno RN (2003) Nutrient budgets and trophic state in a hypersaline coastal lagoon: Lagoa de Araruama. *Estuar Coast Shelf Sci*, Brazil, pp 843–858

- Tomczak M, Godfrey JS (1994) Regional oceanography: an introduction. Pergamon, Oxford
- Tunnell JW Jr, Judd FW (2002) The Laguna Madre of Texas and Tamaulipas. A&M University Press, Texas
- EPA Victoria (2002) Port Phillip Bay water quality. Long-term trends in nutrient status and clarity. 1984–1999. EPA Victoria Publication #806. At: <http://epanote2.epa.vic.gov.au/EPA/publications.nsf/PubDocsLU/806?OpenDocument>. Accessed 27 June 2011
- Whetton P, Power S (2007) Climate change in Australia, technical report. CSIRO and Bureau of Meteorology, ISBN: 9781921232930. At: <http://www.csiro.au/resources/Climate-Change-Technical-Report-2007.html>. Accessed 27 June 2011